


RESEARCH

Open Access



Maintenance of tRNA and elongation factors supports T3SS proteins translational elongations in pathogenic bacteria during nutrient starvation

Yue Sun¹, Xiaolong Shao^{1,2}, Yingchao Zhang¹, Liangliang Han¹, Jiadai Huang¹, Yingpeng Xie¹, Jingui Liu¹ and Xin Deng^{1,3*} 

Abstract

Background: Sufficient nutrition contributes to rapid translational elongation and protein synthesis in eukaryotic cells and prokaryotic bacteria. Fast synthesis and accumulation of type III secretion system (T3SS) proteins conduce to the invasion of pathogenic bacteria into the host cells. However, the translational elongation patterns of T3SS proteins in pathogenic bacteria under T3SS-inducing conditions remain unclear. Here, we report a mechanism of translational elongation of T3SS regulators, effectors and structural protein in four model pathogenic bacteria (*Pseudomonas syringae*, *Pseudomonas aeruginosa*, *Xanthomonas oryzae* and *Ralstonia solanacearum*) and a clinical isolate (*Pseudomonas aeruginosa* UCBPP-PA14) under nutrient-limiting conditions. We proposed a luminescence reporter system to quantitatively determine the translational elongation rates (ERs) of T3SS regulators, effectors and structural protein under different nutrient-limiting conditions and culture durations.

Results: The translational ERs of T3SS regulators, effectors and structural protein in these pathogenic bacteria were negatively regulated by the nutrient concentration and culture duration. The translational ERs in 0.5 × T3SS-inducing medium were the highest of all tested media. In 1 × T3SS-inducing medium, the translational ERs were highest at 0 min and then rapidly decreased. The translational ERs of T3SS regulators, effectors and structural protein were inhibited by tRNA degradation and by reduced levels of elongation factors (EFs).

Conclusions: Rapid translational ER and synthesis of T3SS protein need adequate tRNAs and EFs in nutrient-limiting conditions. Numeric presentation of T3SS translation visually indicates the invasion of bacteria and provides new insights into T3SS expression that can be applied to other pathogenic bacteria.

Keywords: Pathogenic bacteria, T3SS, Translational elongation rate, Nutrient-limiting conditions, tRNA, Elongation factor

Introduction

Bacterial growth primarily depends on protein synthesis catalyzed by the ribosome. Protein accounts for half of the bacterial biomass, and its synthesis requires more than 60% of the total cellular energy [1, 2]. Bacterial growth and survival can be suppressed by many environmental stressors, such as nutrient deficiency, oxidative

*Correspondence: xindeng@cityu.edu.hk

¹ Department of Biomedical Sciences, City University of Hong Kong, Kowloon Tong, Hong Kong SAR, China

Full list of author information is available at the end of the article



© The Author(s) 2022. **Open Access** This article is licensed under a Creative Commons Attribution 4.0 International License, which permits use, sharing, adaptation, distribution and reproduction in any medium or format, as long as you give appropriate credit to the original author(s) and the source, provide a link to the Creative Commons licence, and indicate if changes were made. The images or other third party material in this article are included in the article's Creative Commons licence, unless indicated otherwise in a credit line to the material. If material is not included in the article's Creative Commons licence and your intended use is not permitted by statutory regulation or exceeds the permitted use, you will need to obtain permission directly from the copyright holder. To view a copy of this licence, visit <http://creativecommons.org/licenses/by/4.0/>. The Creative Commons Public Domain Dedication waiver (<http://creativecommons.org/publicdomain/zero/1.0/>) applies to the data made available in this article, unless otherwise stated in a credit line to the data.

stress, low temperatures and high osmotic pressure [3–6]. The bacterial growth rate depends on many factors: the ribosome concentration, the ribosome translational elongation rate (ER) and other factors, such as tRNAs, and ribosome-affiliated factors [1, 7]. Translational elongation comprises four basic steps. In the first step, mRNA codons recognise and regulate tRNAs. In the second step, tRNA is transferred to the ribosome by the elongation factor (EF) Tu. In the third step, the polypeptide chain is assembled with amino acids, catalyzed by tRNA. Finally, the movement of deacylated tRNA results in ribosome translocation [8]. During the translation, ribosomes move at the uneven rates along the mRNAs [9]. The dynamic of translational elongation contributes to the protein folding [10, 11]. Translational elongation is essential to the physiological regulation as the elongation stage consumes great mass of energy for protein synthesis [12]. The unstable translational elongation process can lead to diseases, such as cancers [13, 14]. In bacteria, the fluctuation of translational ER changes the speed of ribosome movement that affects the protein synthesis [15, 16]. Under nutrient-limiting conditions, the protein synthesis rate and bacterial growth are severely inhibited [17, 18].

The activity of the bacterial type III secretion system (T3SS) is regulated by environmental nutrition conditions or the host environment and enables bacterial pathogens to invade host cells [19, 20]. In Gram-negative bacteria such as *Pseudomonas syringae*, *Pseudomonas aeruginosa*, *Xanthomonas oryzae* and *Ralstonia solanacearum*, the highly conserved T3SS is the key factor allowing the establishment of infection. The T3SS needle-like machinery delivers effector proteins into host cells to suppress the host immune system [21, 22]. Bacterial infection of plants results in substantial crop yield losses [23–25], while in humans, bacteria cause several types of infectious diseases [26, 27]. In general, T3SS is suppressed under nutrient-rich conditions but induced under nutrient-poor conditions, such as intercellular spaces [28–30].

Many T3SS regulators have been identified in recent decades [31–34]. In the case of the opportunistic human pathogen *P. aeruginosa*, the T3SS genes are induced by contact with host cells or by low-calcium conditions, which can be achieved by adding 5 mM ethylene glycol tetraacetic acid (EGTA) to LB [35, 36]. The T3SS genes are directly regulated by ExsA, which autoregulates its expression by binding to the promoters and activating their transcription [19]. ExsA transcriptional activation can be inhibited by the anti-activators ExsD and PtrA [37, 38]. PopN is a repressor of T3SS that is the first gene of the operon *popN-PCR1-PCR2-PCR3-PCR4-PCR5-PCR6-PCR7-PCR8-PCR9-PCR10-PCR11-PCR12-PCR13-PCR14-PCR15-PCR16-PCR17-PCR18-PCR19-PCR20-PCR21-PCR22-PCR23-PCR24-PCR25-PCR26-PCR27-PCR28-PCR29-PCR30-PCR31-PCR32-PCR33-PCR34-PCR35-PCR36-PCR37-PCR38-PCR39-PCR40-PCR41-PCR42-PCR43-PCR44-PCR45-PCR46-PCR47-PCR48-PCR49-PCR50-PCR51-PCR52-PCR53-PCR54-PCR55-PCR56-PCR57-PCR58-PCR59-PCR60-PCR61-PCR62-PCR63-PCR64-PCR65-PCR66-PCR67-PCR68-PCR69-PCR70-PCR71-PCR72-PCR73-PCR74-PCR75-PCR76-PCR77-PCR78-PCR79-PCR80-PCR81-PCR82-PCR83-PCR84-PCR85-PCR86-PCR87-PCR88-PCR89-PCR90-PCR91-PCR92-PCR93-PCR94-PCR95-PCR96-PCR97-PCR98-PCR99-PCR100*. PopN contributes

to detecting the intracellular calcium levels [39]. PopN interacts with Pcr1 and suppresses the T3SS expression in *P. aeruginosa* [39, 40].

In plant pathogens, T3SS is encoded by the clustered hypersensitive response (*hrc*) and pathogenicity (*hrp*) genes, which are divided into two groups. Group I includes the *hrp* clusters of *P. syringae*, while group II contains those of *X. oryzae* and *R. solanacearum* [41]. Most T3SS genes are directly regulated by the alternative sigma factor HrpL, which binds to the *hrp* box in the T3SS gene promoter region [42, 43]. *hrpL* transcription is activated through the regulation of another alternative sigma factor, RpoN [44]. *hrpL* transcription is also autoregulated through the bi-directional promoter region between *hrpL* and *hrpJ* [45]. Heterodimerised HrpRS binds to the *hrpL* promoter and activates *hrpL* expression [46]. HrpS can also directly activate the transcription of T3SS genes independent of HrpR [47]. The *hrpRS* gene operon is positively regulated by HrpA, a component of the T3SS pilus, and the extra-cytoplasmic function sigma factor AlgU [48, 49]. HrpRS is modulated by at least six two-component systems (TCSs): RhpRS, CvsRS, GacAS, AauRS, CbrAB2 and EnvZ-OmpR [32, 50–53]. In addition, a variety of regulators positively or negatively modulate T3SS genes. The protease Lon suppresses T3SS by degrading HrpR and other effectors secreted by T3SS [54, 55]. The HrpGVFJ regulatory pathway controls the formation of HrpRS heterodimer at the post-transcriptional level [56–59]. Many transcription factors, such as PilR, TrpI and GntR, act as virulence regulators by influencing T3SS [60]. HrpA2 is one of the major T3SS structural proteins and activates the hypersensitive reaction and pathogenesis in the plants, which shows a significant role in the *P. syringae* pv. *tomato* DC3000 [61]. *hopG1* gene encodes a T3SS effector protein that localizes to the mitochondria. HopG1 promotes the growth of pathogens and inhibits the plant defense responses [62, 63]. T3SS effector HopX1 is a cysteine protease. In *P. syringae* pv. *tabaci*, HopX1 facilitates the susceptibility through directly degrading jasmonate pathway repressors [64, 65].

In *P. syringae*, RhpRS is a master regulatory TCS of T3SS [32, 66]. The *rhpS* and *rhpR* genes are located in the same operon; *rhpS* encodes a histidine kinase and *rhpR* encodes a cognate response regulator [66]. Phosphorylated RhpR directly binds to the *rhpRS* promoter and activates *rhpRS* expression to regulate a group of virulence-related phenotypes [34]. As an important negative response regulator of *hrpRS*, phosphorylated RhpR binds to the *hrpRS* promoter to suppress the *hrpRS-hrpL-hrp* gene cascade under different environmental conditions [31, 32, 34, 67]. RhpS senses changes in environmental conditions and dephosphorylates phosphorylated

RhpR, thereby suppressing *rhpRS* expression [31, 66]. We recently found that RhpS also senses polyphenols to inhibit the expression of T3SS and *P. syringae* virulence [68].

In *X. oryzae*, Hpa1 is an *hrp*-dependent secreted protein that is regulated by two genes, *hrpG* and *hrpX* [69, 70]. HrpX directly activates the expression of *hrp* genes by recognizing the consensus sequence in its promoters [71]. In *R. solanacearum*, HrpG acts as a TCS response regulator that activates the production of plant hormones and regulates the expression of virulence genes involved in bacterial protection responses and plant cell wall degradation [72]. In addition, HrpG positively regulates the transcription of HrpB, which is called HrpX in *X. oryzae* [73].

Although many T3SS regulators have been identified, the translational elongation capacity of T3SS under nutrient-limiting conditions remains uncertain. However, this process plays a considerable role in T3SS protein regulation and bacterial infection. Here, we identified a mechanism in which the T3SS translational ER in four model bacteria is negatively regulated by the nutrient conditions and culture durations. The ER under nutrient-limiting conditions was suppressed by tRNA degradation and reduced levels of EFs. This unified mechanism of T3SS protein translational elongation under nutrient-limiting conditions indicates that such conditions would hinder bacterial infection.

Results

Translation patterns of T3SS regulators, effectors and structural protein of pathogenic bacteria

The translational ER is an accurate indicator for evaluating protein synthesis [4]. Elongation is required for synthesizing proteins under nutrient-limiting conditions in *Escherichia coli*, even though it occurs at a slow rate [74]. However, the translational ERs of T3SS proteins and the associated inhibitory factors in pathogenic bacteria remain unclear. Thus, we evaluated the ERs of T3SS regulators, effectors and structural protein in *P. syringae* (PS), *P. aeruginosa* (PA), *X. oryzae* (XO) and *R. solanacearum* (RS). Here, we constructed two kinds of reporters. One included the corresponding promoter and a promoter-less luciferase (*lux*) in the plasmid, which was the transcriptional fusion reporter to calculate the transcription time ($T_{initiation}$). The other reporter included the corresponding promoter, the coding sequence (CDS) and a promoter-less luciferase (*lux*) in the plasmid, which was the reporter for both transcription and translation to calculate the time for both processes (T_{test}). The translational elongation time (T_{first}) of target protein was calculated by T_{test} minus $T_{initiation}$. The translational ERs

of the tested proteins equaled protein length (L) divided by T_{first} [4, 75].

To test the expression pattern of key T3SS regulators, effectors and structural protein in the four above mentioned pathogenic bacteria under T3SS-inducing ($1 \times$ MM for PS, LB+ 5 mM EGTA for PA, $1 \times$ XOM2 for XO and $1 \times$ MM_{RS} for RS) and T3SS-suppressing conditions ($1 \times$ KB for PS, LB for PA, $1 \times$ M210 for XO and $1 \times$ B for RS), we constructed eight transcriptional and translational fusion reporters containing the full-length CDS of the following T3SS genes: *hrpL*_{PS}, *hopG1*_{PS}, *hrpR*_{PS}, *hopX1*_{PS}, *hrpA2*_{PS}, *popN*_{PA}, *hpa1*_{XO} and *hrpG*_{RS}. As shown in Fig. 1, among these four pathogenic bacteria, T3SS genes were significantly induced by 4–80-fold in the respective T3SS-inducing media but were suppressed in the nutrient-rich media. The expression levels of HrpR_{PS} and PopN_{PA} increased rapidly within the first 3 h in T3SS-inducing conditions (Fig. 1C and F). In contrast, the expression levels of HrpL_{PS}, HopG1_{PS}, HopX1_{PS}, HrpA2_{PS}, Hpa1_{XO} and HrpG_{RS} increased slowly and gradually reached the highest levels within 6–10 h (Fig. 1A, B, D, E, G and H). In addition, we found that the expression levels of HrpL_{PS}, HrpR_{PS}, HopX1_{PS} and PopN_{PA} significantly declined in the lag phase, which might be attributed to the bacteria adapting to the altered nutritional environment (Fig. 1A, C, D and F). As negative controls, non-T3SS proteins (alcohol dehydrogenase, AdhB_{PS}, lysis phenotype activator, AlpA_{PA}, exopolysaccharide xanthan biosynthesis export protein, GumB_{XO}, succinyl-CoA synthetase, SucC_{RS} and) were induced to a high level in the nutrient-rich media (Additional file 1: Fig. S1A–D). To investigate if these perceptions can apply to the clinical isolates, we also detected the expression levels of *popN* in *P. aeruginosa* UCBPP-PA14 (*popN*_{PA14}), a highly virulent and infectious strain [76]. Like PopN_{PA}, PopN_{PA14} was significantly induced by threefold in LB with 5 mM EGTA within the first 3 h, and gradually reduced within the following 7 h (Additional file 1: Fig. S1E). Non-T3SS protein RND multidrug efflux membrane fusion protein, MexA_{PA14}, showed similar trend with that of AlpA_{PA} (Additional file 1: Fig. S1F). For HrpG_{RS}, the expression in MM_{RS} at 50 and 60 min were induced rapidly so that the synthesis time of HrpG_{RS} was not calculated (Additional file 1: Fig. S1G). Taken together, these results indicate that the expression levels of these T3SS regulators, effectors and structural protein showed similar induction patterns with slight differences in the response time in the T3SS-inducing media. The translational ERs of HrpL_{PS}, HopG1_{PS}, HrpR_{PS}, HopX1_{PS} and HrpA2_{PS} under $1 \times$ T3SS-inducing conditions ranged from 8 to 16 aa/s (Fig. 1I). The ERs of PopN_{PA}, Hpa1_{XO} and HrpG_{RS} were ~ 9 aa/s, ~ 1.7 aa/s

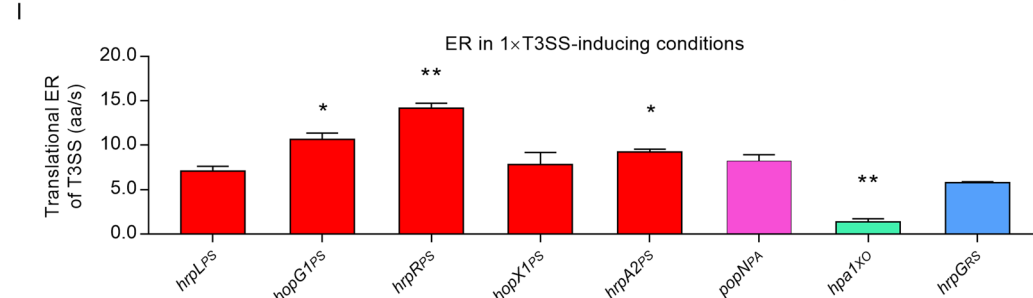
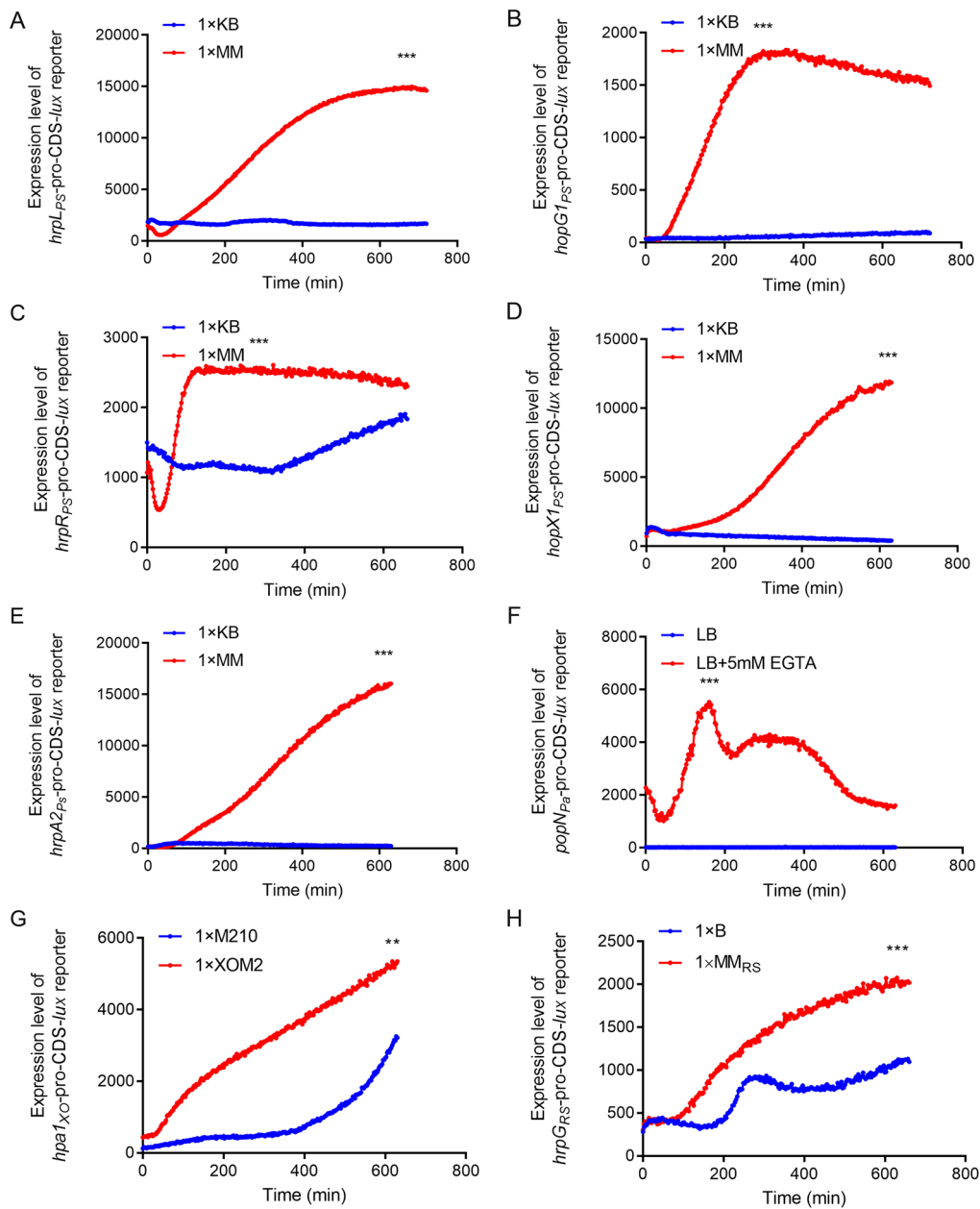


Fig. 1 The expression levels of mentioned T3SS proteins were significantly induced in nutrition-limited medium. **A–H** The expression level of T3SS regulators, effectors and structural protein in four model pathogenic bacteria were measured using the transcriptional fusion reporters in 1 × T3SS-inducing media and 1 × T3SS-suppressing media, including *HrpL_{PS}*, *HopG1_{PS}*, *HrpR_{PS}*, *HopX1_{PS}*, *HrpA2_{PS}*, *PopN_{PS}*, *Hpa1_{XO}* and *HrpG_{RS}*. **I** The translational ERs of the tested T3SS regulators, effectors and structural protein in 1 × T3SS-inducing media and 1 × T3SS-suppressing media. **p* < 0.05; ***p* < 0.01; and ****p* < 0.001. Results were indicated in mean ± SD. All experiments were repeated at least three times

and ~6 aa/s, respectively (Fig. 11). In general, the expression levels of T3SS regulators, effectors and structural protein in these four pathogenic bacteria showed different translational ERs in the T3SS-inducing media.

Nutrient level and culture duration are negatively correlated with the translational ER of T3SS regulators, effectors and structural protein

Because the translational ERs of the T3SS regulators, effectors and structural protein differed among the tested proteins and strains, we hypothesized that the translational ERs might be influenced by the nutritional conditions and culture durations. To quantify the effect of the nutritional condition on the translational ERs, we first evaluated the translational ERs under nutritional conditions that were lower (0.25× and 0.5× T3SS-inducing medium) and higher (2× and 3× T3SS-inducing medium, and 0.5× rich medium) than the normal T3SS-inducing medium (1× T3SS-inducing medium). The results showed that the T3SS translational ERs of PS, XO and RS in 0.5× MM or 0.5× XOM2 were higher (1.5–3-fold for PS, 1.7-fold for XO and fourfold for RS) than those in 1× MM or 1× XOM2 (Fig. 2A, C and D). Although T3SS protein synthesis in 0.5× T3SS-inducing medium was slightly faster than that in 1× T3SS-inducing medium, the expression levels of T3SS regulators, effectors and structural protein in 0.5× T3SS-inducing medium rapidly decreased (Additional file 1: Fig. S2). For PA, the T3SS translational ERs were calculated in LB broth supplemented with different concentrations of EGTA (40 mM, 20 mM, 10 mM, 5 mM and 2.5 mM) to generate a calcium gradient. The maximum translational ER of PopN_{PA} protein occurred at 5 mM EGTA (Fig. 2B). In general, the T3SS translational ERs of these four bacteria dramatically decreased with increasing nutrient levels in the media.

To investigate the influence of culture duration on the T3SS translational ERs, we measured the translational ERs over the first 60 min in 1× T3SS-inducing media. In PS, the translational ERs of T3SS regulators, effectors and structural protein gradually decreased (~90%) from 0 to 16 min after induction and then kept at a low level, showing a time-course behaviour (Fig. 2E). The translational ERs of T3SS regulators and effectors in PA, XO and RS were similar to those in PS (Fig. 2E–H). For PA14, the translational ER of PopN_{PA14} distinctly decreased with the EGTA concentration and culture duration (Additional file 1: Fig. S3A, B). Regarding the translational ERs of non-T3SS proteins (negative controls), the MexA_{PA14} ERs had no significant difference under different EGTA concentrations and at various culture duration (Additional file 1: Fig. S3C–E). The translational ER of AdhB_{PS} under nutrient-rich

conditions (~8.5 aa/s) was higher than that in the 2× rich medium and nutrient-limiting medium (less than 1.5 aa/s) (Additional file 1: Fig. S3F). Moreover, the translational ER of AdhB_{PS} in KB at 0 min was eightfold higher than at other points (less than 1.0 aa/s), and all the AdhB_{PS} ERs in MM were low, with no significant differences among them (0.16–0.39 aa/s) (Additional file 1: Fig. S3G, H). These results indicate that the AdhB_{PS} ER was not correlated with culture duration. For PA, the ERs of AlpA_{PA} in LB (~13.5 aa/s) were also higher than those found in medium supplemented with EGTA (0.4–3.5 aa/s) (Additional file 1: Fig. S3I). The AlpA_{PA} ERs in LB at 0–40 min (greater than 10 aa/s) were higher than those at 50 and 60 min (~2.1 aa/s and ~4.0 aa/s, respectively), and were less than 1.0 aa/s in LB supplemented with EGTA (Additional file 1: Fig. S3J and K). For XO, the translational ER of Gumb_{XO} in 1× M210 (~0.5 aa/s) had no significant differences with those in 0.5× M210 and 0.125× M210 (~0.8 aa/s). The ERs at 10, 30, 40 and 50 min (~0.7–0.8 aa/s) showed no differences with that at 0 min (~0.5 aa/s) apart from those at 20 and 60 min (~0.9–1.0 aa/s) (Additional file 1: Fig. S3L and M). Similarly, for RS, the translational ERs of SucC_{RS} in 0.5×, 0.25× and 0.125× B (~0.9–1.4 aa/s) were much lower than that in 1× B (~13.4 aa/s). The translational ERs for 10–60 min (~1.3–2.7 aa/s) were much lower than that at 0 min (~13.4 aa/s) (Additional file 1: Fig. S3N and O). In general, the translational ERs of T3SS regulators, effectors and structural protein were negatively correlated with the nutrient level and culture duration.

Translational ERs of T3SS regulators, effectors and structural protein were independent on the mRNA transcription

The first step of translational elongation is the recognition and regulation of cognate tRNAs, which is carried out by mRNA codons [8]. The mRNA synthesis levels can change in accordance with the cell cycle [77, 78]. To investigate the influence of mRNA synthesis on the translational ER of T3SS regulators, effectors and structural protein, we assessed the induction kinetics of T3SS gene mRNAs in the transcriptional and translational fusion reporters of four pathogenic bacteria over the first 30 min in T3SS-inducing medium using qRT-PCR with reverse primers at the 3' end. As shown in Fig. 3, the expression levels of full-length T3SS mRNAs were strongly induced under nutrient-limiting conditions. The initial synthesis time of these T3SS regulators, effectors and structural protein showed similar patterns of requiring approximately 2000 s (red lines in Fig. 3). However, the transcription durations of the T3SS mRNAs showed different kinetics trends. Among them, *hrpL*_{PS} and *hopG1*_{PS} mRNA transcription required

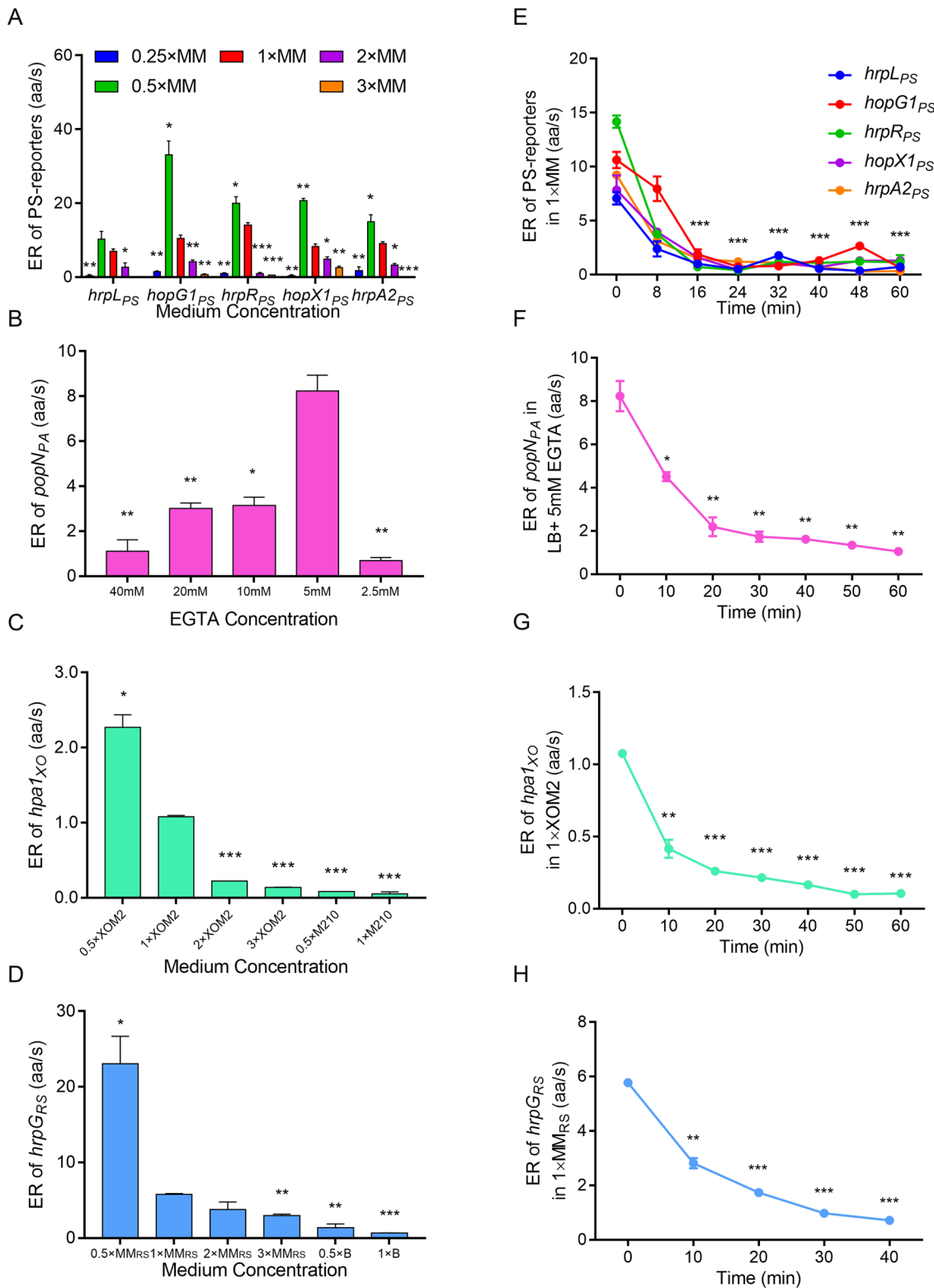


Fig. 2 Translational ERs of mentioned T3SS proteins were dependent on the nutrient doses and culture time. **A–H** Translational ERs of T3SS regulators, effectors and structural protein (*HrpL_{PS}*, *HopG1_{PS}*, *HrpR_{PS}*, *HopX1_{PS}*, *HrpA2_{PS}*, *PopN_{PA}*, *Hpa1_{XO}*, and *HrpG_{RS}*) under different nutrition-limited conditions and at various culture time (0–60 min). The standard deviations were shown but were very small in the plot. * $p < 0.05$; ** $p < 0.01$; and *** $p < 0.001$. Results were indicated in mean \pm SD. All experiments were repeated at least three times

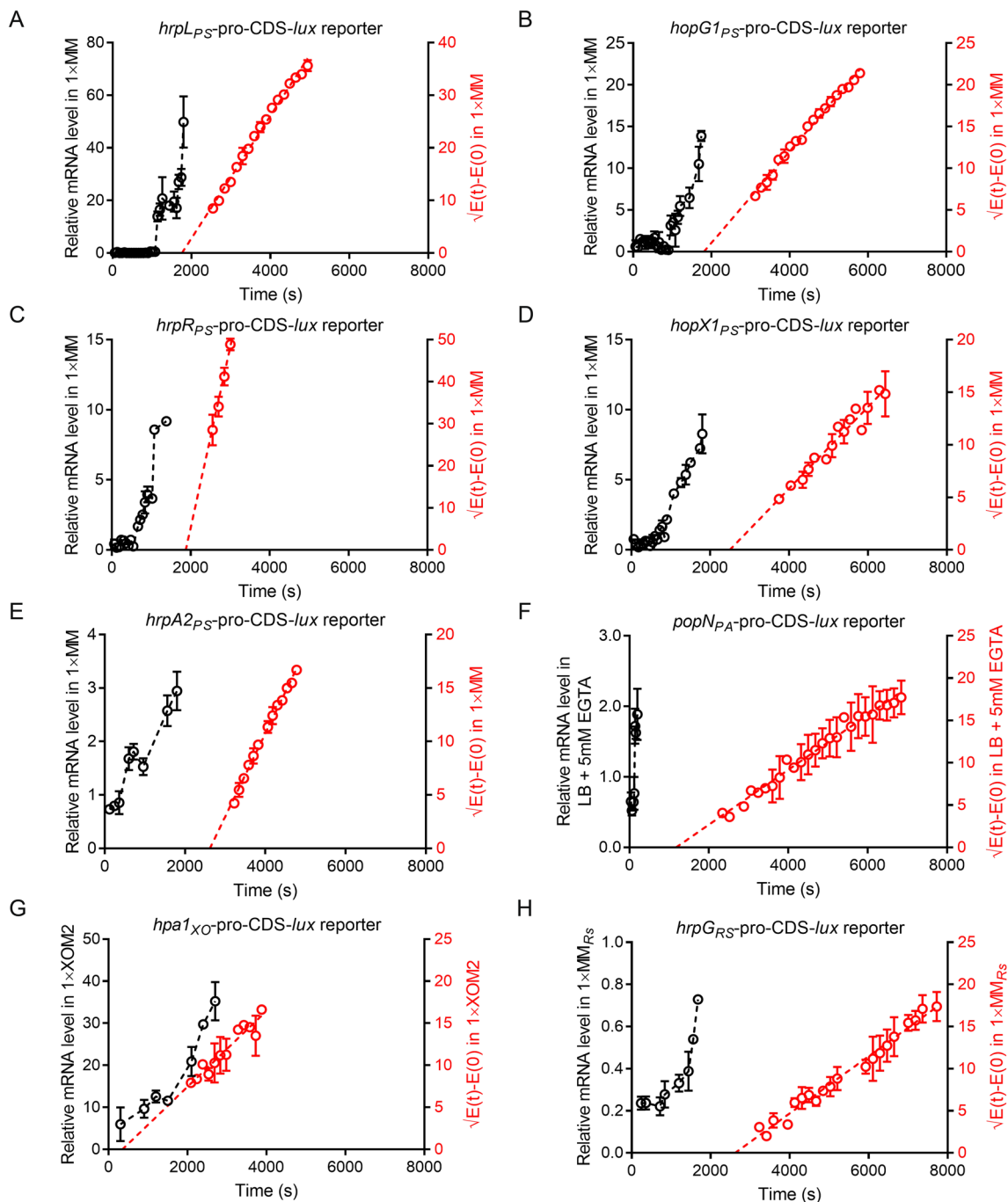


Fig. 3 The first T3SS full-length protein synthesis back the full-length mRNA synthesis under $1 \times$ T3SS-inducing conditions. **A–H** Induction assay of full-length T3SS mRNAs (*hrpL_{PS}*, *hopG1_{PS}*, *hrpR_{PS}*, *hopX1_{PS}*, *hrpA2_{PS}*, *popN_{PA}*, *hpa1_{XO}* and *hrpG_{RS}*) of transcriptional and translational fusion reporters which were induced in $1 \times$ T3SS-inducing conditions. The qRT-PCR primers were used to detect the 3' end region of T3SS mRNAs. qRT-PCR detected the synthesis kinetics of full-length T3SS mRNAs. The Schleif plots ($\sqrt{E(t) - E(0)}$) of all T3SS mRNAs were shown in red. The standard deviations were shown but were very small in the plot. All experiments were repeated at least three times

~ 1080 s and ~ 900 s, which were shorter than the initial first full-length protein syntheses (~ 1769 s and ~ 1830 s, respectively) (Fig. 3A and B). The mRNA synthesis

durations of other T3SS regulators, effectors and structural protein were less than ~ 540 s (Fig. 3C–H). Notably, the full-length mRNAs of *hrpA2_{PS}*, *popN_{PA}* and *hpa1_{XO}*

were rapidly synthesized (~ 480 s, ~ 140 s and ~ 300 s) (Fig. 3E–G), while the first full-length protein syntheses began at ~ 2485 s, ~ 1178 s and ~ 350 s, respectively. For clinical strain, the transcription level of *popN*_{PA14} mRNA was rapidly induced at ~ 360 s in LB with 5 mM EGTA, much shorter than the initial first full-length PopN_{PA14} syntheses (~ 2191 s) (Additional file 1: Fig. S4A). For non-T3SS proteins, the *adhB*_{PS} mRNA level in MM gradually declined throughout 7 h of culture, while the translation duration of AdhB_{PS} was longer than 5 h (Additional file 1: Fig. S4B). In contrast, in PA and PA14, the full-length mRNA of *alpA*_{PA} and *mexA*_{PA14} were rapidly synthesised (~ 15 min and ~ 10 min), leading to their translation at ~ 47.8 min and ~ 4.9 min (Additional file 1: Fig. S4C and D). These results indicate that protein synthesis began when the full-length mRNA level of T3SS genes was sufficiently high, demonstrating that under nutrient-limiting conditions, the translational ERs of T3SS regulators, effectors and structural protein were independent on the mRNA synthesis levels.

Cellular tRNA levels positively affect the translational elongation of T3SS proteins in the latter culture period

Because the translational ER is also related to cellular tRNA levels [1], we hypothesized that the reduced translational ERs during the first 60 min of culture might be caused by the tRNA levels. To verify this hypothesis, we quantitatively characterised the tRNA levels of transcriptional and translational fusion reporters of the four tested bacteria using the different culturing conditions and durations. Most of the 20 tested tRNAs displayed a similar tendency. As expected, the tRNA levels of RS were decreased by $\sim 40\%$ at 40 min compared with those at 0 min (Fig. 4J–L), which correlated with the reduced translational ERs of HrpG_{RS} (Fig. 2H). The tRNA-Ile level had rapidly decreased by $\sim 80\%$ at 10 min and by $\sim 90\%$ at 20 min (Fig. 4J). Compared with 0 min, the tRNA-Tyr level at 20 min had declined by $\sim 80\%$ (Fig. 4K).

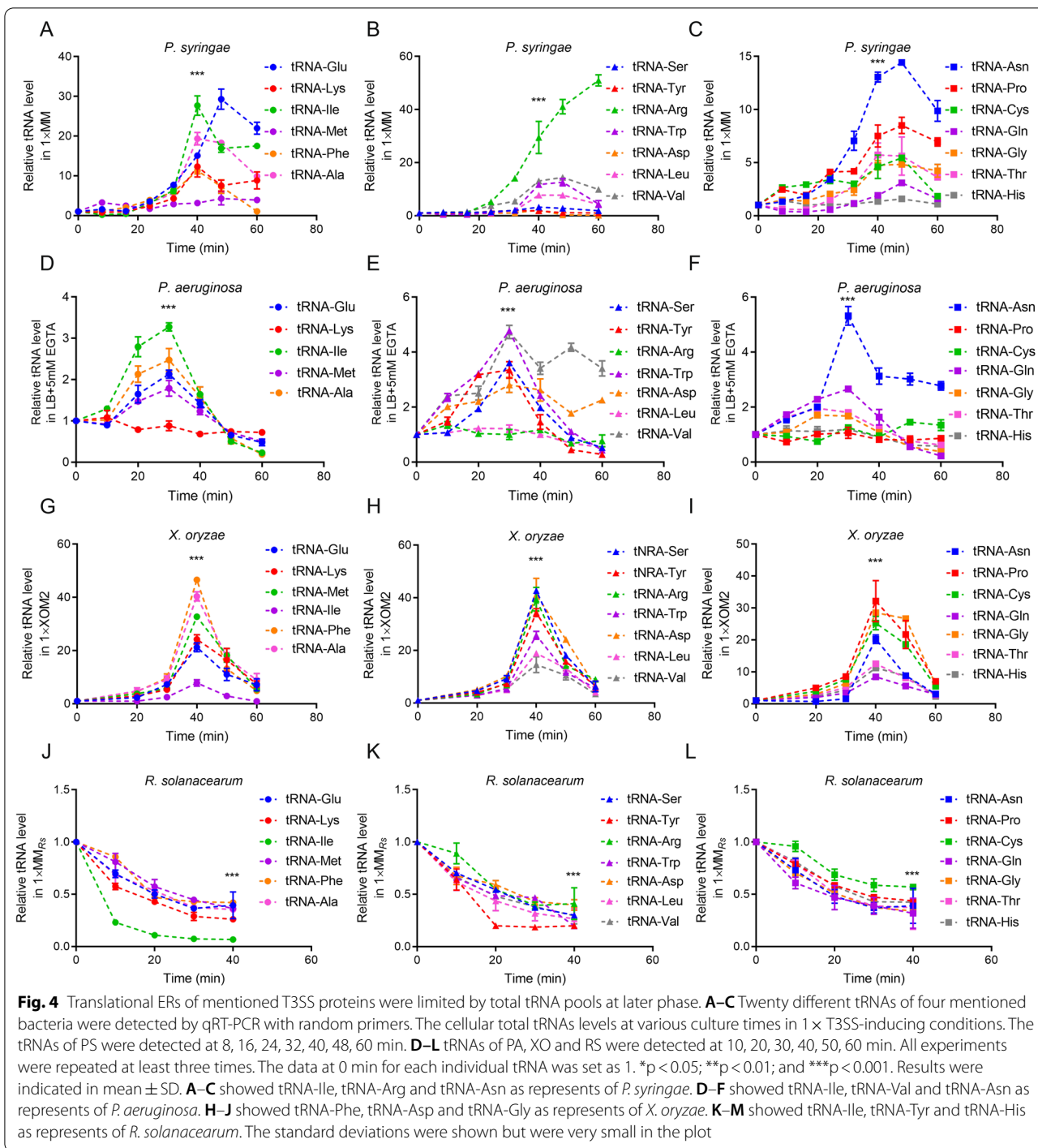
The tRNA expression patterns showed different trends in other bacteria. In PS, although the tRNA expression levels significantly increased with the culture duration under T3SS-inducing conditions, the expression of most tested tRNAs had decreased after 48 min (Fig. 4A–C). The tRNA-Glu and tRNA-Asn expression levels were greater than tenfold higher than those at the beginning of induction, and the level of tRNA-Arg was 50-fold higher than that at 0 min. We also found that the expression levels of tRNA-Ile, tRNA-Ala and tRNA-Lys had declined at 40 min. The expression levels of tRNA-Met, tRNA-Tyr, tRNA-Ser and tRNA-His showed no significant variations throughout the induction. For PA, the expression levels of most tRNAs peaked at 30 min and

then decreased (Fig. 4D–F). The levels of tRNA-Trp, tRNA-Val and tRNA-Asn increased by \sim fivefold (Fig. 4E and F). Unlike other tRNAs that decreased to their initial level at 60 min, the expression levels of tRNA-Val, tRNA-Asp and tRNA-Asn at 60 min were \sim two–threefold higher than those at 0 min (Fig. 4E and F). However, the expression levels of tRNA-Lys, tRNA-Arg, tRNA-Leu, tRNA-Pro, tRNA-Cys and tRNA-His were stable throughout the 60-min culture. For PA14, most of the 20 tested tRNAs represented the highly increase within the first 20–30 min and the gradually decline in the following 30–40 min, like tRNA-Ile (Additional file 1: Fig. S5A–C). For XO, tRNA expression peaked at 40 min (Fig. 4G–I), followed by a rapid decrease to the initial levels by 60 min. Taken together, these results indicated that the tRNA expression levels showed trends similar to those of the corresponding translational ERs under T3SS-inducing conditions in the latter culture period.

EFs positively regulate the translational elongations of T3SS regulators, effectors and structural protein

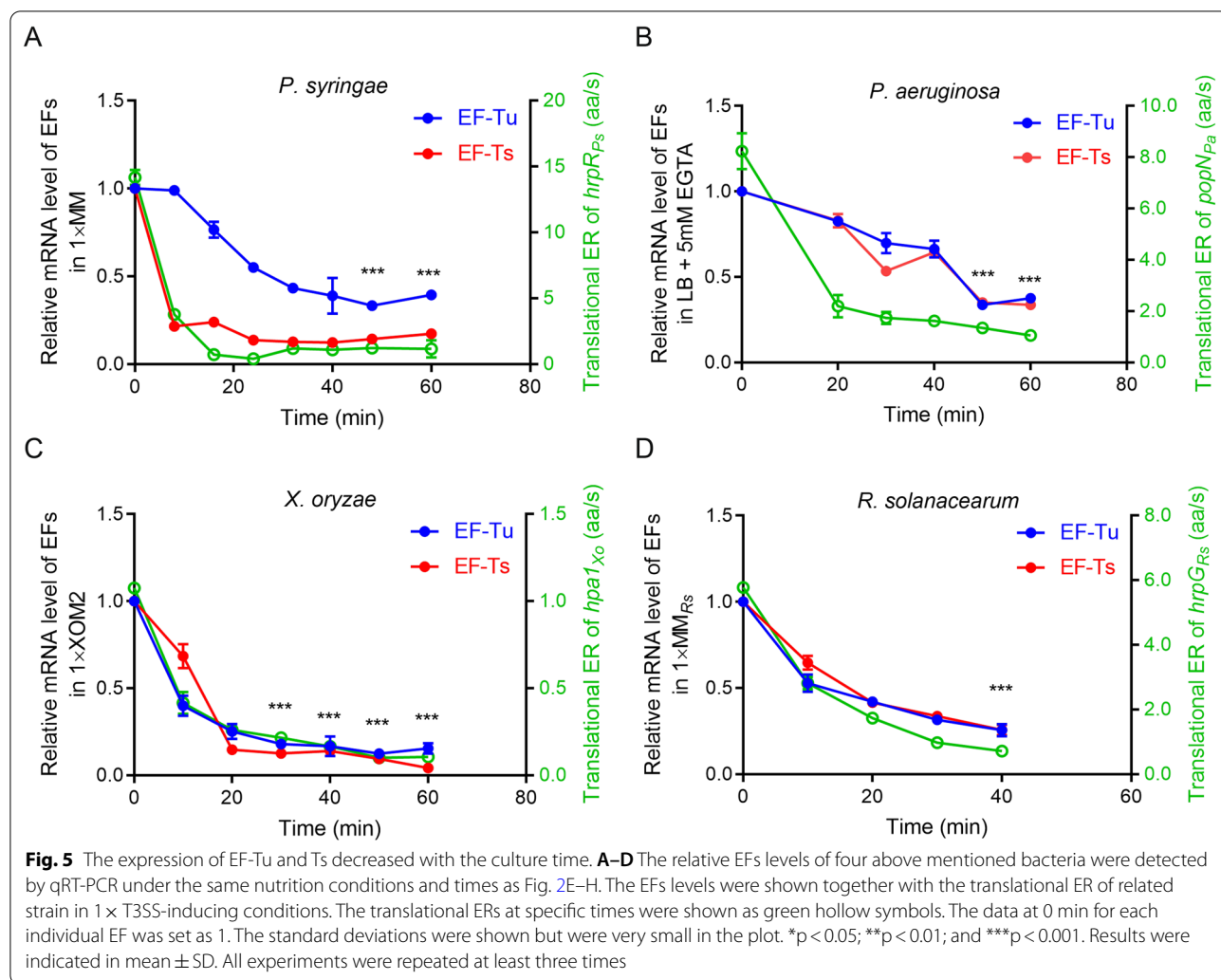
EF-Tu and EF-Ts play critical roles in polypeptide elongation [79]. To further understand the translational elongation patterns of T3SS regulators, effectors and structural protein in the tested pathogenic bacteria, we detected the expression levels of EF-Tu and EF-Ts under the different culture conditions and at various culture durations. In PS (Fig. 5A), the EF-Tu level gradually declined and at 60 min was reduced by $\sim 40\%$ compared with 0 min. Compared with EF-Tu, at 8 min, the expression level of EF-Ts was decreased by $\sim 85\%$. Similar to the HrpR_{PS} translational ER (solid green line in Fig. 5A), EF-Ts expression level remained low throughout the 16–60 min of culture. In XO, EF-Tu expression level was reduced by $\sim 60\%$ at 10 min and by $\sim 85\%$ at 60 min, while the expression level of EF-Ts was decreased by $\sim 40\%$ at 10 min and by $\sim 90\%$ at 60 min.

In contrast, in XO, the reduced translational ER of Hpa1_{XO} was more consistent with the EF-Tu level (Fig. 5C). In RS, the trends in these two EF levels were similar, showing an $\sim 75\%$ decrease at 60 min, which was similar to the trend for the HrpG_{RS} translational ER. We also found that the translational ERs of PS, PA and RS decreased to a greater extent (by $\sim 90\%$) than the respective EFs (by $\sim 60\%$) in nutrient-limiting conditions (Fig. 5A, B and D). Different from relative expression levels of EFs of the model pathogenic bacteria at 10 min (less than 1), the relative expression levels of EFs of PA14 were high up to 7. Even at 40 min, the relative expression level of EF-Tu was still as high as 1.6. The high expression of EFs of PA14 provided support to the fast translational ER



and conducted to the high virulence (Additional file 1: Fig. S5D). The translational ERs of these five bacteria decreased by more than 90% after 60 min of culture, while the EF levels had reduced by 70–90% at 60 min (Fig. 5 and Additional file 1: Fig S5). Overall, similar

trends in the translational ERs and EF levels indicated that EF-Tu and EF-Ts play important roles on the translational elongation of T3SS regulators, effectors and structural protein under nutrient-limiting conditions.



Discussion

Rapid T3SS protein synthesis is vital for the invasion of pathogenic bacteria. However, the patterns of T3SS protein translation have not been elucidated. In prokaryotes, variations in *E. coli* translational elongation have been studied [80–83]. Initiation of mRNA translation, but not the concentration of tRNAs, is a rate-limiting step for protein synthesis under nutrient-rich conditions [16, 84]. In environments with low carbon and nitrogen availability, the ERs in *E. coli* gradually decrease, but they remain constant in rich conditions [74, 81, 85]. In contrast, our data suggested that the translational ERs of T3SS in pathogenic bacteria steadily declined with increasing nutrient concentrations and culture time. Although maintaining a low ER in the later period of incubation, T3SS proteins gradually accumulated. Rapid ER of T3SS proteins in the early incubation reflected the instantaneous response of pathogenic bacteria to environmental change. In addition, we demonstrated that

the T3SS translational ERs decreased with the prolongation of culture duration. These results indicate that both the total tRNA and the EF levels are constraints on the translational elongation of T3SS regulators, effectors and structural protein. In the latter culture period, the degradation of total tRNAs and the gradual reduction of EF levels restricted the T3SS translational ERs. These findings reveal key aspects of T3SS translational ERs in pathogenic bacteria under nutrient-limiting conditions.

The results showed that the reduced translational ERs were caused by decreasing tRNA levels in the latter culture period (Fig. 4). From 30–40 to 60 min of culture, the reduction in tRNAs was consistent with the decrease in translational ERs (Fig. 2E–H). A model of tRNA degradation suggests that tRNAs degrade with early amino acid starvation in *E. coli*, which is in-line with the reduced demand for protein and the improved quality in protein synthesis [86]. In addition, the charge level of tRNAs rapidly decreases during early starvation

and the reduced number of charged tRNAs inhibits the translational elongation of T3SS. In the present study, total tRNAs in PS, PA and XO quickly accumulated from 0–30 to ~40 min of culture. Studies have shown that tRNA accumulation results in cells death [87]. Accumulating tRNAs can result in the incorrect insertion of an amino acid into a polypeptide, leading to a decrease translational ER [88]. As mRNA transcription also plays an important role on the T3SS expression under nutrient starvation, we calculated the transcriptional ERs of T3SS regulators, effectors and structural protein in the four mentioned pathogenic bacteria (Table 1). Compared with the translational ERs, the transcriptional ERs were much lower, indicating the significant effect of translational ER on T3SS protein synthesis.

In Table 1, we defined the time of mRNA production as T_{mRNA} and unified the unit as 3 nt/s. Therefore, the transcriptional ER was calculated as $L_m/3T_{mRNA}$, which L_m was the length of each full-length mRNA. Results are indicated in mean \pm SD. All experiments were repeated at least three times.

In addition to increasing tRNA levels, we found that reduced EF levels also resulted in decreased translational ERs of T3SS regulators, effectors and structural protein under nutrient-limiting conditions. Charged tRNAs move to the ribosome as a ternary complex with GTP and EF-Tu; this complex can be hydrolyzed and released as EF-Tu-GDP [89]. GDP is reactivated to GTP through a sequence of nucleotide exchanges carried out by EF-Tu-Ts complexes [79]. Our results showed that the EF levels had rapidly decreased by ~60% after 40 min in nutrient-limiting conditions (Fig. 5), suggesting their positive regulation of the T3SS translational ERs. The ribosome concentration is strongly affected by the EF-Ts concentration whereby a high EF-Ts level facilitates rapid cell growth [90, 91]. Therefore, the reduced EF levels of the four bacteria suggest that few ternary complexes participate in T3SS translation under

nutrient-limiting conditions, causing the decreased translational ERs (Fig. 5).

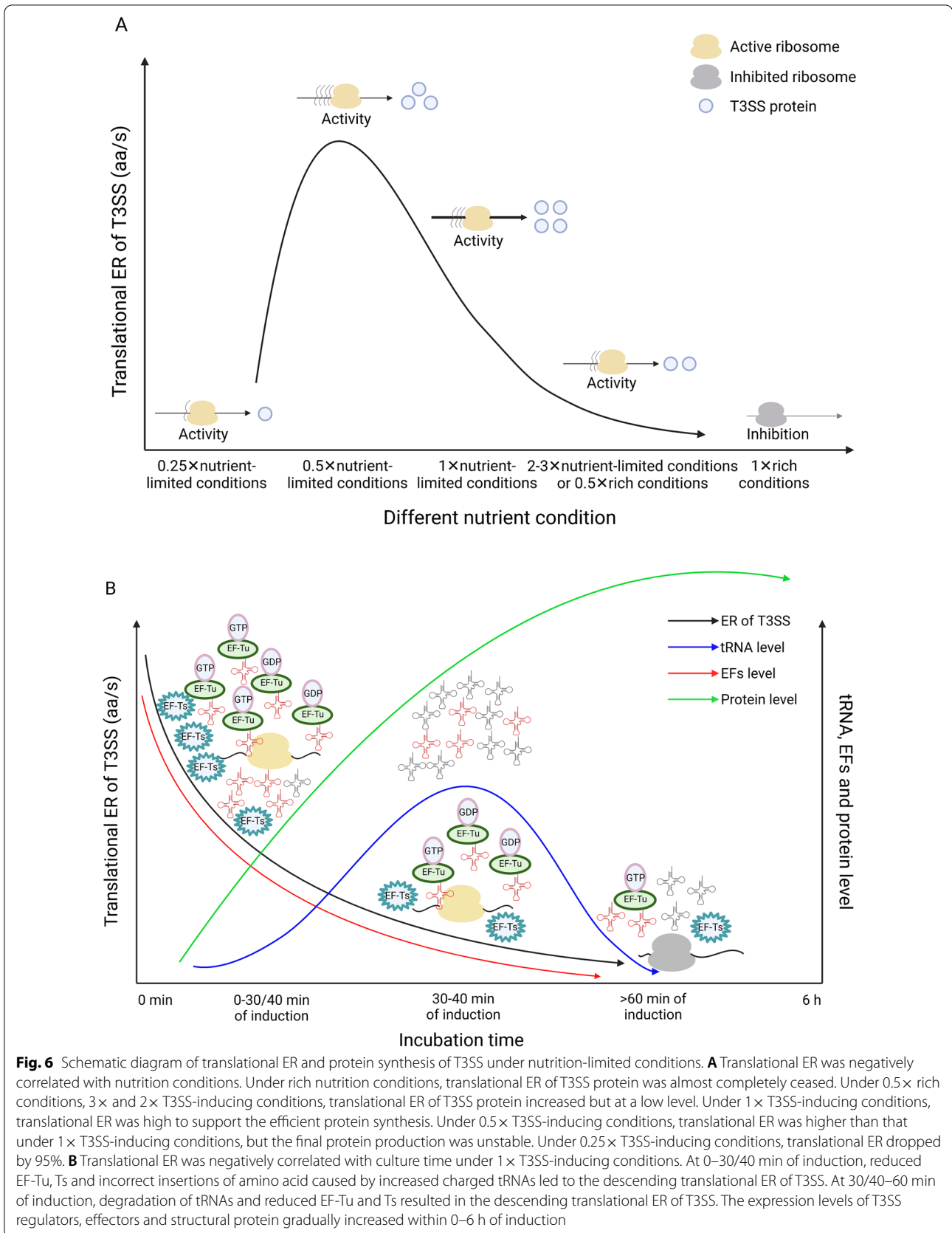
To better understand the virulence of the tested pathogens, we detected the relative expression level of the tested T3SS genes during the first 0–6 h after induction. As shown in Additional file 1: Fig. S6A–E, the expression levels of *hrpL_{PS}*, *hpa1_{XO}* and *hrpG_{RS}* markedly increased during 0–6 h-induction. For *popN_{PA}* and *popN_{PA14}*, the expression levels enhanced during 0–3 h and then gradually reduced in the following 3 h. As a repressor of T3SS, the decrease of the transcription of *popN* contributed to the invasion of T3SS to the host. The qRT-PCR result revealed the dynamic change of T3SS genes after induction.

Based on the results of this study, we propose a model in which the levels of tRNAs and EFs regulate translational ERs under nutrient-limiting conditions. The translational ERs were negatively correlated with the nutrient concentration. As shown in Fig. 6A, the expression level of T3SS regulators, effectors and structural protein was low under nutrient-rich conditions. Under 0.5 \times nutrient-rich conditions and 3 \times and 2 \times T3SS-inducing conditions, the T3SS translational ERs slightly increased but remained low. In the 1 \times T3SS-inducing condition, the T3SS translational ERs rapidly increased and supported a high amount of protein synthesis. Under the 0.5 \times T3SS-inducing condition, the translational ERs were higher than those under the 1 \times T3SS-inducing condition, but the final amount of protein production varied. Under the 0.25 \times T3SS-inducing condition, the translational ERs rapidly decreased. Figure 6B shows that the incubation duration negatively regulated the translational ERs under the 1 \times T3SS-inducing condition. From 0–30 to ~40 min of induction, the decreasing T3SS translational ERs were caused by the reduced EF levels. From 30–40 to 60 min of induction, tRNAs degradation and reduced EF levels resulted in decreasing T3SS translational ERs. The expression level of T3SS regulators, effectors and structural protein gradually increased within 6 h of induction and was then stably maintained.

In conclusion, our study elucidated that tRNAs and EFs play important roles in regulating the translational ERs of T3SS regulators, effectors and structural protein. We characterized the T3SS translational ERs based on a luminescence reporter system, which quantitatively illustrated the translational elongation pattern of T3SS under nutrient-limiting conditions. Different but fast ERs of various T3SS proteins in the early incubation numerically emphasize the multiple response of pathogenic bacteria to environmental change. Our findings provide insights into the

Table 1 T3SS transcriptional ERs were much lower than the T3SS translational ERs in 1 \times T3SS-inducing media

Tested proteins	Transcriptional ER (3 nt/s)	Translational ER (aa/s)
HrpL _{PS}	0.17 \pm 0.01	7.08 \pm 0.57
HopG1 _{PS}	0.56 \pm 0.03	10.63 \pm 0.74
HrpR _{PS}	0.54 \pm 0.04	14.18 \pm 0.56
HopX1 _{PS}	0.67 \pm 0.05	8.41 \pm 0.55
HrpA2 _{PS}	0.28 \pm 0.03	9.24 \pm 0.33
PopN _{PA}	2.01 \pm 0.57	8.24 \pm 0.7
Hpa1 _{XO}	0.43 \pm 0.05	1.08 \pm 0.02
HrpG _{RS}	0.64 \pm 0.04	5.78 \pm 0.12



quantitative translational of T3SS and the significance of tRNAs, EF-Tu and EF-Ts on T3SS translational elongation under nutrient-limiting conditions. These findings in four model pathogenic bacteria might apply to other bacterial species.

Experimental procedures

Bacterial strains, plasmid and primers

The bacterial strains used in this study were wild-type *P. syringae* (PS) 1448A, *P. aeruginosa* (PA) PAO1, *P. aeruginosa* UCBPP-PA14 (PA14) PA14, *X. oryzae* (XO) PXO99A and *R. solanacearum* (RS) OE 1-1. The tested genes were *hrpL*_{PS}, *hopG1*_{PS}, *hrpR*_{PS}, *hopX1*_{PS}, *hrpA2*_{PS}, *adhB*_{PS}, *popN*_{PA}, *alpA*_{PA}, *popN*_{PA14}, *mexA*_{PA14}, *hpa1*_{XO}, *gumB*_{XO}, *hrpG*_{RS} and *sucC*_{RS}. The pMS402 plasmid was used [34], which encodes a promoter-less luciferase (*lux*). The bacterial strains, plasmid and primers are listed in Table S1 in the Additional file 1. Each T3SS gene included two reporters. One included the corresponding promoter and a promoter-less luciferase (*lux*) in the plasmid, which was the transcriptional fusion reporter. The other reporter concluded the corresponding promoter, the coding sequence (CDS) and a promoter-less luciferase (*lux*) in the plasmid, which was the transcriptional and translational fusion reporter.

Cell growth conditions

PS 1448A, XO PXO99A and RS OE 1-1 were grown in the nutrient-rich media King'B (KB) [92], M210 [93] and B [94], respectively at 28°C until reaching an optical density at 600 nm (OD₆₀₀) of ~0.6. PA PAO1 and PA14 were cultured in LB at 37 °C. For PS, XO and RS, the pre-culture was centrifuged, washed three times, and resuspended in distilled water. For the induction curve, the *lux* activity of the final experimental culture at OD₆₀₀ ~0.1 in the T3SS-inducing condition was immediately measured. The nutrient-limiting media were MM for PS (50 mM KH₂PO₄, 7.6 mM (NH₄)₂SO₄, 1.7 mM MgCl₂, 1.7 mM NaCl, and 10 mM fructose, pH 5.7) [95], XOM2 for XO (0.18% xylose sugar, 670 μM D, L-methionine, 10 mM sodium L(+)-glutamate, 14.7 mM KH₂PO₄, 40 μM MnSO₄, 240 μM Fe(III) EDTA and 5 mM MgCl₂, pH 6.5) [96] and MM_{RS} for RS [97], respectively. To investigate different nutrient conditions, nutrient gradients of the media were used to induce nutrient-limiting conditions. For the PA and PA14 pre-culture, 5 mM EGTA and 100 mM MgCl₂ were added to induce T3SS gene expression, and various doses of EGTA and MgCl₂ were used to achieve a range of calcium stress conditions. Related parameters including the translational ER and the mRNA, tRNA and EF levels were measured at specific time points. The kanamycin concentrations were 100 μg/mL for PS and 50 μg/mL for XO and RS. The

trimethoprim concentration was 50 μg/mL for PA and PA14.

Translational ER measurement

The measurement and calculation of the translational ER were based on a luminescence reporter system and a LacZ induction assay, respectively [4, 75]. Therefore, we constructed two kinds of reporters. One included the corresponding gene promoter and a promoter-less luciferase (*lux*) in the plasmid, which was the transcriptional reporter to calculate the transcription time ($T_{initiation}$). The other reporter concluded the corresponding promoter, the CDS and a promoter-less luciferase (*lux*) in the plasmid, which was the reporter for both transcription and translation to calculate the time for both processes (T_{test}). The synthesis cost of the promoters was assessed as the initiation time, and the associated calibrations are described in Additional file 1: Fig. S7. Immediately after transferring into the investigated media (for PS, XO and RS) or after the addition of EGTA and MgCl₂ (for PA and PA14), the *lux* activity was measured using a microplate reader (600 nm excitation filter) at 2.5-min intervals. The induction curve of the tested proteins was constructed by plotting the *lux* activity against the induction time and analysed with a Schleif plot. We considered $E(0)$ as the basal *lux* activity of the reporter and $E(t)$ as the *lux* activity at the specific time point of induction. $\sqrt{E(t) - E(0)}$ is positively correlated with time [98]; therefore, the x-intercept of the Schleif plot is the time needed for translating one molecule. T_{test} was regarded as the intact cost time, and $T_{initiation}$ was regarded as the initiation cost time. The synthesis time of the first round of the tested proteins, T_{first} could thus be calculated as:

$$T_{first} = T_{test} - T_{initiation} \quad (1)$$

Therefore, the translational ER can be calculated as:

$$ER = L / (T_{test} - T_{initiation}) \quad (2)$$

where L is the length of each full-length protein.

The $\sqrt{E(t) - E(0)}$ values of Hpa1_{XO} and HrpG_{RS} were showed in Additional file 1: Fig. S8.

Measuring mRNA, tRNA and EF abundances by qRT-PCR

The mRNA, tRNA and EF abundances were measured by quantitative reverse transcription (qRT-PCR). The qRT-PCR primers used are shown Table S1 in the Additional file 1. To measure the transcriptional kinetics of the full-length T3SS mRNAs, the transcriptional and translational fusion reporters were grown to OD₆₀₀ ~0.6 and then transferred into the investigated media. Immediately after induction, 500 μL of culture was removed at 1-min intervals and added to 500 μL of pre-cooled stop

solution containing 60% ethanol, 2% phenol and 10 mM EDTA. The total RNA purification of PS, PA, PA14 and XO was performed with a RNeasy mini kit (Qiagen); the RS total RNA was isolated using TRIzol reagent (Invitrogen). The RNA concentrations were measured using a NanoDrop 2000 spectrophotometer (ThermoFisher). cDNA synthesis was performed using HiScript III RT SuperMix (Vazyme, China). qRT-PCR was performed with a SuperReal Premix Plus (SYBR Green) kit (Tiangen Biotech) according to the manufacturer's instructions. The relative mRNA abundance at each time point was $2^{Ct(0)-Ct(t)}$, where $Ct(0)$ indicates the Ct value of the sample taken immediately before transfer to nutrient-limiting conditions, and $Ct(t)$ indicates the Ct value at each time point thereafter. The relative mRNA synthesis level was plotted against time to obtain the transcriptional kinetics curve.

To measurement the relative tRNA and EF levels, 500 μ L of culture was removed at 8-min (PS) or 10-min (PA, PA14, XO and RS) intervals and centrifuged at 12,000 rpm for 1 min to harvest the bacteria. The RNA purification and reverse transcription processes were performed as previously mentioned, except the total RNA was incubated at 80 °C for 15 min before cDNA synthesis to remove the secondary structure of tRNA. The corresponding 16S rRNAs of PS, PA and PA14, *gyrB* of XO and *serC* of RS were used as internal references. Relative expression levels of tRNAs and EFs at various time points were calculated by the $2^{-(\Delta\Delta Ct)}$ method.

Supplementary Information

The online version contains supplementary material available at <https://doi.org/10.1186/s13578-022-00884-6>.

Additional file 1: Figure S1. Induction curves of PopN_{PA14} and non-T3SS proteins (AdhB_{PS}, AlpA_{PA}, MexA_{PA14}, Gumb_{XO} and SucC_{RS}) induced in 1 × T3SS-inducing conditions and 1 × T3SS-repressing conditions. **(A)** The red curve showed the delayed expression levels of *adhB_{PS}-pro-CDS-lux* reporter in 1 × MM compared with that in 1 × KB. **(B)** The red curve showed the slightly fast expression levels of *alpA_{PA}-pro-CDS-lux* reporter in LB + 5 mM EGTA compared with that in LB. **(C)** The red curve showed the delayed expression levels of *gumb_{XO}-pro-CDS-lux* reporter in 1 × XOM2 compared with that in 1 × M210. **(D)** The red curve showed the delayed expression levels of *sucC_{RS}-pro-CDS-lux* reporter in 1 × MM_{RS} compared with that in 1 × B. **(E)** The red curve showed the slightly fast expression levels of *popN_{PA14}-pro-CDS-lux* reporter in LB + 5 mM EGTA compared with that in LB. **(F)** The red curve showed the slightly fast expression levels of *mexA_{PA14}-pro-CDS-lux* reporter in LB + 5 mM EGTA compared with that in LB. **(G)** The expression of HrpG_{RS} in MM_{RS} at 50 and 60 min were induced rapidly so that the synthesis time of HrpG_{RS} was not calculated. **Figure S2.** Expression levels of T3SS regulators, effectors and structural protein of *P. syringae*, *X. oryzae* and *R. solanacearum* in 0.5 × T3SS-inducing conditions were less stable than that in 1 × T3SS-inducing conditions. The red curve and green curve denoted the expression levels in 1 × and 0.5 × T3SS-inducing conditions, respectively. **(A)** The expression levels of *hrpL_{PS}-pro-CDS-lux* reporter were extremely low in 0.5 × MM compared with those in 1 × MM. **(B-D, F)** The expression levels of *hopG1_{PS}*, *hrpR_{PS}*, *hopX1_{PS}* and *hrpG_{RS}-pro-CDS-lux* reporters in 0.5 × T3SS-inducing conditions rapidly increased, but declined to a low level immediately

compared with those in 1 × T3SS-inducing conditions. **(E)** The expression levels of *hpa1_{XO}-pro-CDS-lux* reporter in 0.5 × XOM2 were slightly lower than those in 1 × XOM2. **Figure S3.** Translational elongation rate of PopN_{PA14} and non-T3SS proteins (AdhB_{PS}, AlpA_{PA}, MexA_{PA14}, Gumb_{XO} and SucC_{RS}) in multiple nutrition conditions and at various time. **(A-B)** Translational ERs of PopN_{PA14} under different EGTA concentrations and at various culture time (0–60 min). **(C)** The translational ERs of MexA_{PA14} in LB with EGTA (~1.0–2.2 aa/s) were much lower than that in LB (~5.2 aa/s) with no significant difference. **(D-E)** The translational ERs of MexA_{PA14} in both LB and LB with 5 mM EGTA during various culture times kept at a low level (~0.5–2.0 aa/s and ~0.8–1.8 aa/s, respectively). **(F)** The translational ER of AdhB_{PS} in 1 × MM (~8 aa/s) was more than fourfold than those in richer or poorer nutrition conditions (less than 2 aa/s). **(G)** In 1 × KB, the translational ER of AdhB_{PS} at the beginning of culture (~8 aa/s) had significant difference than those at various culture time (less than 2 aa/s). **(H)** In 1 × MM, the translational ERs of AdhB_{PS} at 0–4 h of culture were much lower than that in 1 × KB, which had no difference. **(I)** The translational ER of AlpA_{PA} in LB (~13 aa/s) was more than threefold than those in LB + EGTA (less than 5 aa/s). **(J)** In LB, the translational ERs of AlpA_{PA} at 0–40 min of culture (10–15 aa/s) had no difference. The ER decreased rapidly at 50–60 min (less than 5 aa/s). **(K)** In LB + 5 mM EGTA, the translational ERs of AlpA_{PA} were much lower than those in LB. **(L)** The translational ER of Gumb_{XO} in 1 × M210 (~0.5 aa/s) had no significant differences with those in 0.5 × M210 and 0.125 × M210 (~0.8 aa/s). **(M)** The translational ERs of Gumb_{XO} at 10, 30, 40 and 50 min (~0.7–0.8 aa/s) showed no differences with that at 0 min (~0.5 aa/s) apart from those at 20 and 60 min (~0.9–1.0 aa/s). **(N)** The ERs of SucC_{RS} in 0.5 × , 0.25 × and 0.125 × B (~0.9–1.4 aa/s) were much lower than that in 1 × B (~13.4 aa/s). **(O)** The translational ERs of SucC_{RS} for 10–60 min (~1.3–2.7 aa/s) were much lower than that at 0 min (~13.4 aa/s). **Figure S4.** Induction assay of full-length PopN_{PA14} and non-T3SS proteins (AdhB_{PS}, AlpA_{PA} and MexA_{PA14}) mRNAs in 1 × T3SS-inducing conditions. **(A)** The mRNA synthesis level of *popN_{PA14}* was rapidly induced in LB with 5 mM EGTA. $\sqrt{E(t) - E(0)}$ plot showed that T_{test} of PopN_{PA14} was ~2191 s in LB with 5 mM EGTA. **(B)** The mRNA synthesis level of *adhB_{PS}* rapidly decreased in 1 × MM and maintained a low level within 26–420 min. $\sqrt{E(t) - E(0)}$ plot showed that T_{test} of AdhB_{PS} was ~343.7 min in 1 × MM. **(C)** The mRNA synthesis level of *alpA_{PA}* increased after adding EGTA and dropped to the starting level. $\sqrt{E(t) - E(0)}$ plot showed that T_{test} of AlpA_{PA} was ~47 s in LB + 5 mM EGTA. **(D)** The mRNA synthesis level of *mexA_{PA14}* increased after adding EGTA and dropped to the starting level. $\sqrt{E(t) - E(0)}$ plot showed that T_{test} of MexA_{PA14} was ~5 min in LB + 5 mM EGTA. **Figure S5.** Relative expression levels of tRNAs and EFs of PA14 in LB with 5 mM EGTA. **(A-C)** tRNAs of PA14 were detected at 10, 20, 30, 40, 50, 60 min. The data at 0 min for each individual tRNA was set as 1. **(D)** The relative EFs levels of PA14 were detected by qRT-PCR. The EFs levels were shown together with the translational ER of PopN_{PA14} in LB with 5 mM EGTA. The translational ERs at specific times were shown as green hollow symbols. The standard deviations were shown but were very small in the plot. * $p < 0.05$; ** $p < 0.01$; and *** $p < 0.001$. Results were indicated in mean \pm SD. All experiments were repeated at least three times. **Figure S6.** The expression levels of T3SS genes during 0–6-h inducing culture. **(A-E)** The expression levels of *hrpL_{PS}*, *popN_{PA14}*, *hpa1_{XO}*, *hrpG_{RS}* and *popN_{PA14}* in 1 × T3SS-inducing conditions for 0–6 h. **Figure S7.** The Schleif plot of T3SS regulators, effectors and structural protein of *P. syringae*, *P. aeruginosa*, *X. oryzae* and *R. solanacearum* in 1 × T3SS-inducing conditions. The Schleif plot was used to detect the translational time of the first newly synthesized protein in 1 × T3SS-inducing conditions. The square root of newly synthesized protein ($\sqrt{E(t) - E(0)}$) was linear correlated with time during the initial dozens of minutes. $E(t)$ denoted the expression levels of the tested proteins at specific times in 1 × T3SS-inducing conditions, and $E(0)$ denoted the basal expression levels of the culture. The green line and red line described the linear line of transcriptional fusion reporters and reporters containing both transcription and translation, respectively. The x-intercepts of the green line and red line denoted the time for the initial cost ($T_{initiation}$) and the transcription and translation of the tested proteins (T_{test}), respectively. Therefore, the difference of the two intercepts corresponded to the time to translate the full-length protein molecule

(T_{first}). The initial cost included the sense of cells to nutrient conditions, RNA polymerase transcriptional initiation and ribosome translational initiation (Ref. 4 of the main text). The initiation time of various proteins were different (~ 1702 s for HrpL_{PS}, ~ 1791 s for HopG1_{PS}, ~ 1699 s for HrpR_{PS}, ~ 2454 s for HopX1_{PS}, ~ 2485 s for HrpA2_{PS}, ~ 759.8 s for PopN_{PA}, ~ 17.03 s for Hpa1_{XO} and ~ 2553 s for HrpG_{RS}). **Figure S8.** T_{test} s of Hpa1_{XO} and HrpG_{RS} in 1 × T3SS-repressing conditions were much longer than those in 1 × T3SS-inducing conditions. The red line and blue line denoted the time containing both transcription and translation (T_{test}) in 1 × T3SS-inducing conditions and 1 × T3SS-repressing conditions, respectively. **(A)** T_{test} s of *hpa1*_{XO}-pro-CDS-*lux* reporter in 1 × XOM2 and 1 × M210 were ~ 3.352 min and ~ 300.4 min. **(B)** T_{test} s of *hrpG*_{RS}-pro-CDS-*lux* reporter in 1 × MM_{RS} and 1 × B medium were ~ 42.35 s and ~ 181.2 s. **Table S1.** Bacterial strains, plasmid, and primers used in this study.

Acknowledgements

Not applicable.

Author contributions

XD and YS designed experiments. YS performed experiments. YZ and LH helped to construct the reporters. JH, YX, JL and XS helped to analyze data. XD, XS and YS wrote the manuscript. All authors discussed the results and contributed to the manuscript. All authors read and approved the final manuscript.

Funding

This work is supported by General Research Fund of Hong Kong (11102720, 21103018, 11101619 and 11103221 to Xin Deng), National Natural Science Foundation of China (31870116 and 32172358 to Xin Deng).

Availability of data and materials

All data generated or analysed during this study are included in this published article and its additional files.

Declarations

Ethics approval and consent to participate

Not applicable.

Consent for publication

Not applicable.

Competing interests

The authors declare that they have no competing interests.

Author details

¹Department of Biomedical Sciences, City University of Hong Kong, Kowloon Tong, Hong Kong SAR, China. ²College of Plant Protection, Laboratory of Plant Immunity, Key Laboratory of Integrated Management of Crop Diseases and Pests, Nanjing Agricultural University, No. 1 Weigang, Nanjing 210095, Jiangsu, China. ³Shenzhen Research Institute, City University of Hong Kong, Shenzhen 518057, China.

Received: 4 June 2022 Accepted: 13 August 2022

Published online: 05 September 2022

References

- Klumpp S, Scott M, Pedersen S, Hwa T. Molecular crowding limits translation and cell growth. *Proc Natl Acad Sci*. 2013;110(42):16754–9.
- Basan M, Zhu M, Dai X, Warren M, Sévin D, Wang YP, et al. Inflating bacterial cells by increased protein synthesis. *Mol Syst Biol*. 2015;11(10):836.
- Zhu M, Dai X. Maintenance of translational elongation rate underlies the survival of *Escherichia coli* during oxidative stress. *Nucleic Acids Res*. 2019;47(14):7592–604.
- Zhu M, Dai X, Wang Y-P. Real time determination of bacterial in vivo ribosome translation elongation speed based on LacZa complementation system. *Nucleic Acids Res*. 2016;44(20):e155.
- Brennan FP, Grant J, Botting CH, O'Flaherty V, Richards KG, Abram F. Insights into the low-temperature adaptation and nutritional flexibility of a soil-persistent *Escherichia coli*. *FEMS Microbiol Ecol*. 2013;84(1):75–85.
- Record MT Jr, Courtenay ES, Cayley DS, Guttman HJ. Responses of *E. coli* to osmotic stress: large changes in amounts of cytoplasmic solutes and water. *Trends Biochem Sci*. 1998;23(4):143–8.
- Dennis PP, Ehrenberg M, Bremer H. Control of rRNA synthesis in *Escherichia coli*: a systems biology approach. *Microbiol Mol Biol Rev*. 2004;68(4):639–68.
- Richter JD, Collier J. Pausing on polyribosomes: make way for elongation in translational control. *Cell*. 2015;163(2):292–300.
- Pedersen S. *Escherichia coli* ribosomes translate in vivo with variable rate. *EMBO J*. 1984;3(12):2895–8.
- Zhang G, Hubalewska M, Ignatova Z. Transient ribosomal attenuation coordinates protein synthesis and co-translational folding. *Nat Struct Mol Biol*. 2009;16(3):274–80.
- Rosano GL, Ceccarelli EA. Rare codon content affects the solubility of recombinant proteins in a codon bias-adjusted *Escherichia coli* strain. *Microb Cell Fact*. 2009;8(1):1–9.
- Proud CG. Regulation and roles of elongation factor 2 kinase. *Biochem Soc Trans*. 2015;43(3):328–32.
- Faller WJ, Jackson TJ, Knight JR, Ridgway RA, Jamieson T, Karim SA, et al. mTORC1-mediated translational elongation limits intestinal tumour initiation and growth. *Nature*. 2015;517(7535):497–500.
- Jan A, Janssonius B, Delaidelli A, An YA, Ferreira N, Smits LM, et al. Activity of translation regulator eukaryotic elongation factor-2 kinase is increased in Parkinson disease brain and its inhibition reduces alpha synuclein toxicity. *Acta Neuropathol Commun*. 2018;6(1):1–17.
- Shah P, Ding Y, Niemczyk M, Kudla G, Plotkin JB. Rate-limiting steps in yeast protein translation. *Cell*. 2013;153(7):1589–601.
- Subramaniam AR, Zid BM, O'Shea EK. An integrated approach reveals regulatory controls on bacterial translation elongation. *Cell*. 2014;159(5):1200–11.
- Vogel U, Sørensen M, Pedersen S, Jensen KF, Kilstrup M. Decreasing transcription elongation rate in *Escherichia coli* exposed to amino acid starvation. *Mol Microbiol*. 1992;6(15):2191–200.
- Iyer S, Le D, Park BR, Kim M. Distinct mechanisms coordinate transcription and translation under carbon and nitrogen starvation in *Escherichia coli*. *Nat Microbiol*. 2018;3(6):741–8.
- Yahr TL, Wolfgang MC. Transcriptional regulation of the *Pseudomonas aeruginosa* type III secretion system. *Mol Microbiol*. 2006;62(3):631–40.
- Tang X, Xiao Y, Zhou J-M. Regulation of the type III secretion system in phytopathogenic bacteria. *Mol Plant Microbe Interact*. 2006;19(11):1159–66.
- Cunnac S, Lindeberg M, Collmer A. *Pseudomonas syringae* type III secretion system effectors: repertoires in search of functions. *Curr Opin Microbiol*. 2009;12(1):53–60.
- Guo M, Tian F, Wamboldt Y, Alfano JR. The majority of the type III effector inventory of *Pseudomonas syringae* pv. *tomato* DC3000 can suppress plant immunity. *Mol Plant Microbe Interact*. 2009;22(9):1069–80.
- González AJ, Landera E, Mendoza MC. Pathovars of *Pseudomonas syringae* causing bacterial brown spot and halo blight in *Phaseolus vulgaris* L. are distinguishable by ribotyping. *Appl Environ Microbiol*. 2000;66(2):850–4.
- Verma G, Mondal KK, Kulshreshtha A, Sharma M. XopRT3SS-effector of *Xanthomonas oryzae* pv. *oryzae* suppresses cell death-mediated plant defense response during bacterial blight development in rice. *3 Biotech*. 2019;9(7):1–10.
- Peeters N, Guidot A, Vaillau F, Valls M. *Ralstonia solanacearum*, a widespread bacterial plant pathogen in the post-genomic era. *Mol Plant Pathol*. 2013;14(7):651–62.
- Richards MJ, Edwards JR, Culver DH, Gaynes RP. Nosocomial infections in medical intensive care units in the United States. *Crit Care Med*. 1999;27(5):887–92.

27. Richards MJ, Edwards JR, Culver DH, Gaynes RP, System NNIS. Nosocomial infections in combined medical-surgical intensive care units in the United States. *Infect Control Hosp Epidemiol*. 2000;21(8):510–5.
28. Hikichi Y, Yoshimochi T, Tsujimoto S, Shinohara R, Nakaho K, Kanda A, et al. Global regulation of pathogenicity mechanism of *Ralstonia solanacearum*. *Plant Biotechnol*. 2007;24(1):149–54.
29. Kanda A, Yasukochi M, Ohnishi K, Kiba A, Okuno T, Hikichi Y. Ectopic expression of *Ralstonia solanacearum* effector protein PopA early in invasion results in loss of virulence. *Mol Plant Microbe Interact*. 2003;16(5):447–55.
30. Shen D-K, Filopon D, Chaker H, Boullanger S, Derouazi M, Polack B, et al. High-cell-density regulation of the *Pseudomonas aeruginosa* type III secretion system: implications for tryptophan catabolites. *Microbiology*. 2008;154(8):2195–208.
31. Deng X, Lan L, Xiao Y, Kennelly M, Zhou J-M, Tang X. *Pseudomonas syringae* two-component response regulator RhpR regulates promoters carrying an inverted repeat element. *Mol Plant Microbe Interact*. 2010;23(7):927–39.
32. Deng X, Liang H, Chen K, He C, Lan L, Tang X. Molecular mechanisms of two-component system RhpRS regulating type III secretion system in *Pseudomonas syringae*. *Nucleic Acids Res*. 2014;42(18):11472–86.
33. Jovanovic M, James EH, Burrows PC, Rego FG, Buck M, Schumacher J. Regulation of the co-evolved HrpR and HrpS AAA+ proteins required for *Pseudomonas syringae* pathogenicity. *Nat Commun*. 2011;2(1):1–9.
34. Xie Y, Shao X, Zhang Y, Liu J, Wang T, Zhang W, et al. *Pseudomonas savastanoi* two-component system RhpRS switches between virulence and metabolism by tuning phosphorylation state and sensing nutritional conditions. *MBio*. 2019. <https://doi.org/10.1128/mBio.02838-18>.
35. Frank DW. The exoenzyme S regulon of *Pseudomonas aeruginosa*. *Mol Microbiol*. 1997;26(4):621–9.
36. Vallis AJ, Yahr TL, Barbieri JT, Frank DW. Regulation of ExoS production and secretion by *Pseudomonas aeruginosa* in response to tissue culture conditions. *Infect Immun*. 1999;67(2):914–20.
37. Dasgupta N, Lykken GL, Wolfgang MC, Yahr TL. A novel anti-anti-activator mechanism regulates expression of the *Pseudomonas aeruginosa* type III secretion system. *Mol Microbiol*. 2004;53(1):297–308.
38. Ha UH, Kim J, Badrane H, Jia J, Baker HV, Wu D, et al. An *in vivo* inducible gene of *Pseudomonas aeruginosa* encodes an anti-ExsA to suppress the type III secretion system. *Mol Microbiol*. 2004;54(2):307–20.
39. Sundin C, Thelau J, Bröms JE, Forsberg Å. Polarisation of type III translocation by *Pseudomonas aeruginosa* requires PcrG, PcrV and PopN. *Microb Pathog*. 2004;37(6):313–22.
40. Yang H, Shan Z, Kim J, Wu W, Lian W, Zeng L, et al. Regulatory role of PopN and its interacting partners in type III secretion of *Pseudomonas aeruginosa*. *J Bacteriol*. 2007;189(7):2599–609.
41. Alfano JR, Collmer A. The type III (Hrp) secretion pathway of plant pathogenic bacteria: trafficking harpins, Avr proteins, and death. *J Bacteriol*. 1997;179(18):5655–62.
42. Xiao Y, Hutcheson SW. A single promoter sequence recognized by a newly identified alternate sigma factor directs expression of pathogenicity and host range determinants in *Pseudomonas syringae*. *J Bacteriol*. 1994;176(10):3089–91.
43. Lam HN, Chakravarthy S, Wei H-L, BuiNguyen H, Stodghill PV, Collmer A, et al. Global analysis of the HrpL regulon in the plant pathogen *Pseudomonas syringae* pv. *tomato* DC3000 reveals new regulon members with diverse functions. *PLoS ONE*. 2014;9(8):e106115.
44. Hendrickson EL, Guevera P, Ausubel FM. The alternative sigma factor RpoN is required for hrpActivity in *Pseudomonas syringae* pv. *Maculicola* and acts at the level of hrpL transcription. *J Bacteriol*. 2000;182(12):3508–16.
45. Waite C, Schumacher J, Jovanovic M, Bennett M, Buck M. Negative autogenous control of the master type III secretion system regulator HrpL in *Pseudomonas syringae*. *MBio*. 2017;8(1):e02273–e2316.
46. Hutcheson SW, Bretz J, Sussan T, Jin S, Pak K. Enhancer-binding proteins HrpR and HrpS interact to regulate hrp-encoded type III protein secretion in *Pseudomonas syringae* strains. *J Bacteriol*. 2001;183(19):5589–98.
47. Wang J, Shao X, Zhang Y, Zhu Y, Yang P, Yuan J, et al. HrpS is a global regulator on type III secretion system (T3SS) and non-T3SS genes in *Pseudomonas savastanoi* pv. *phaseolicola*. *Mol Plant Microbe Interact*. 2018;31(12):1232–43.
48. Wei W, Plovianich-Jones A, Deng W-L, Jin Q-L, Collmer A, Huang H-C, et al. The gene coding for the Hrp pilus structural protein is required for type III secretion of Hrp and Avr proteins in *Pseudomonas syringae* pv. *tomato*. *Proc Natl Acad Sci*. 2000;97(5):2247–52.
49. Markel E, Stodghill P, Bao Z, Myers CR, Swingle B. AlgU controls expression of virulence genes in *Pseudomonas syringae* pv. *tomato* DC3000. *J Bacteriol*. 2016;198(17):2330–44.
50. Chatterjee A, Cui Y, Yang H, Collmer A, Alfano JR, Chatterjee AK. GacA, the response regulator of a two-component system, acts as a master regulator in *Pseudomonas syringae* pv. *tomato* DC3000 by controlling regulatory RNA, transcriptional activators, and alternate sigma factors. *Mol Plant Microbe Interact*. 2003;16(12):1106–17.
51. Fishman MR, Zhang J, Bronstein PA, Stodghill P, Filiatrault MJ. Ca²⁺-induced two-component system CvsSR regulates the type III secretion system and the extracytoplasmic function sigma factor AlgU in *Pseudomonas syringae* pv. *tomato* DC3000. *J Bacteriol*. 2018;200(5):e00538-17.
52. Yan Q, Rogan CJ, Pang Y-Y, Davis EW, Anderson JC. Ancient co-option of an amino acid ABC transporter locus in *Pseudomonas syringae* for host signal-dependent virulence gene regulation. *PLoS Pathog*. 2020;16(7):e1008680.
53. Shao X, Tan M, Xie Y, Yao C, Wang T, Huang H, et al. Integrated regulatory network in *Pseudomonas syringae* reveals dynamics of virulence. *Cell Rep*. 2021;34(13): 108920.
54. Bretz J, Losada L, Lisboa K, Hutcheson SW. Lon protease functions as a negative regulator of type III protein secretion in *Pseudomonas syringae*. *Mol Microbiol*. 2002;45(2):397–409.
55. Hua C, Wang T, Shao X, Xie Y, Huang H, Liu J, et al. *Pseudomonas syringae* dual-function protein Lon switches between virulence and metabolism by acting as both DNA-binding transcriptional regulator and protease in different environments. *Environ Microbiol*. 2020;22(7):2968–88.
56. Wei CF, Deng WL, Huang HC. A chaperone-like HrpG protein acts as a suppressor of HrpV in regulation of the *Pseudomonas syringae* pv. *syringae* type III secretion system. *Mol Microbiol*. 2005;57(2):520–36.
57. Ortiz-Martín I, Thwaites R, Mansfield JW, Beuzón CR. Negative regulation of the Hrp type III secretion system in *Pseudomonas syringae* pv. *phaseolicola*. *Mol Plant Microbe Interact*. 2010;23(5):682–701.
58. Huang YC, Lin YC, Wei CF, Deng WL, Huang HC. The pathogenicity factor HrpF interacts with HrpA and HrpG to modulate type III secretion system (T3SS) function and t3ss expression in *Pseudomonas syringae* pv. *averhoi*. *Mol Plant Pathol*. 2016;17(7):1080–94.
59. Xie Y, Shao X, Deng X. Regulation of type III secretion system in *Pseudomonas syringae*. *Environ Microbiol*. 2019;21(12):4465–77.
60. Fan L, Wang T, Hua C, Sun W, Li X, Grunwald L, et al. A compendium of DNA-binding specificities of transcription factors in *Pseudomonas syringae*. *Nat Commun*. 2020;11(1):1–11.
61. Preston G, Huang H-C, He SY, Collmer A. The HrpZ proteins of *Pseudomonas syringae* pvs. *syringae*, *glycinea*, and *tomato* are encoded by an operon containing *Yersinia ysc* homologs and elicit the hypersensitive response in tomato but not soybean. *Mol Plant Microbe Interact*. 1995;8(5):717–32.
62. Rodríguez-Puerto C, Chakraborty R, Singh R, Rocha-Loyola P, Rojas CM. The *Pseudomonas syringae* type III effector HopG1 triggers necrotic cell death that is attenuated by AtNHR2B. *Sci Rep*. 2022;12(1):1–14.
63. Block A, Guo M, Li G, Elowsky C, Clemente TE, Alfano JR. The *Pseudomonas syringae* type III effector HopG1 targets mitochondria, alters plant development and suppresses plant innate immunity. *Cell Microbiol*. 2010;12(3):318–30.
64. Gimenez-Ibanez S, Boter M, Fernández-Barbero G, Chini A, Rathjen JP, Solano R. The bacterial effector HopX1 targets JAZ transcriptional repressors to activate jasmonate signaling and promote infection in *Arabidopsis*. *PLoS Biol*. 2014;12(2): e1001792.
65. Yang L, Teixeira PJPL, Biswas S, Finkel OM, He Y, Salas-Gonzalez I, et al. *Pseudomonas syringae* type III effector HopBB1 promotes host transcriptional repressor degradation to regulate phytohormone responses and virulence. *Cell Host Microbe*. 2017;21(2):156–68.
66. Xiao Y, Lan L, Yin C, Deng X, Baker D, Zhou J-M, et al. Two-component sensor RhpS promotes induction of *Pseudomonas syringae* type III secretion system by repressing negative regulator RhpR. *Mol Plant Microbe Interact*. 2007;20(3):223–34.

67. Zhou T, Chen K, Zhang H-X, Deng X. Genome-wide DNA binding pattern of two-component system response regulator RhpR in *Pseudomonas syringae*. *Genomics data*. 2015;4:146–7.
68. Xie Y, Ding Y, Shao X, Yao C, Li J, Liu J, et al. *Pseudomonas syringae* senses polyphenols via phosphorelay crosstalk to inhibit virulence. *EMBO Rep*. 2021. <https://doi.org/10.15252/embr.202152805>.
69. Wengelnik K, Rossier O, Bonas U. Mutations in the regulatory gene *hrpG* of *Xanthomonas campestris* pv. *vesicatoria* result in constitutive expression of all *hrp* genes. *J Bacteriol*. 1999;181(21):6828–31.
70. Furutani A, Tsuge S, Oku T, Tsuno K, Inoue Y, Ochiai H, et al. Hpa1 secretion via type III secretion system in *Xanthomonas oryzae* pv. *oryzae*. *J Gen Plant Pathol*. 2003;69(4):271–5.
71. Koebnik R, Krüger A, Thieme F, Urban A, Bonas U. Specific binding of the *Xanthomonas campestris* pv. *vesicatoria* AraC-type transcriptional activator HrpX to plant-inducible promoter boxes. *J Bacteriol*. 2006;188(21):7652–60.
72. Aldon D, Brito B, Boucher C, Genin S. A bacterial sensor of plant cell contact controls the transcriptional induction of *Ralstonia solanacearum* pathogenicity genes. *EMBO J*. 2000;19(10):2304–14.
73. Valls M, Genin S, Boucher C. Integrated regulation of the type III secretion system and other virulence determinants in *Ralstonia solanacearum*. *PLoS Pathog*. 2006;2(8): e82.
74. Dai X, Zhu M, Warren M, Balakrishnan R, Patsalo V, Okano H, et al. Reduction of translating ribosomes enables *Escherichia coli* to maintain elongation rates during slow growth. *Nat Microbiol*. 2016;2(2):1–9.
75. Andersson DI, Bohman K, Isaksson LA, Kurland CG. Translation rates and misreading characteristics of *rpsD* mutants in *Escherichia coli*. *Mol Genet MGG*. 1982;187(3):467–72.
76. Wiehlmann L, Wagner G, Cramer N, Siebert B, Gudowius P, Morales G, et al. Population structure of *Pseudomonas aeruginosa*. *Proc Natl Acad Sci*. 2007;104(19):8101–6.
77. Stumpf CR, Moreno MV, Olshen AB, Taylor BS, Ruggero D. The translational landscape of the mammalian cell cycle. *Mol Cell*. 2013;52(4):574–82.
78. Tanenbaum ME, Stern-Ginossar N, Weissman JS, Vale RD. Regulation of mRNA translation during mitosis. *Elife*. 2015;4: e07957.
79. Hu X-P, Dourado H, Schubert P, Lercher MJ. The protein translation machinery is expressed for maximal efficiency in *Escherichia coli*. *Nat Commun*. 2020;11(1):1–10.
80. Zhang G, Ignatova Z. Generic algorithm to predict the speed of translational elongation: implications for protein biogenesis. *PLoS ONE*. 2009;4(4): e5036.
81. Young R, Bremer H. Polypeptide-chain-elongation rate in *Escherichia coli* B/r as a function of growth rate. *Biochem J*. 1976;160(2):185–94.
82. Zhang G, Fedyunin I, Miekley O, Valleriani A, Moura A, Ignatova Z. Global and local depletion of ternary complex limits translational elongation. *Nucleic Acids Res*. 2010;38(14):4778–87.
83. Sunohara T, Jojima K, Tagami H, Inada T, Aiba H. Ribosome stalling during translation elongation induces cleavage of mRNA being translated in *Escherichia coli*. *J Biol Chem*. 2004;279(15):15368–75.
84. Jacques N, Dreyfus M. Translation initiation in *Escherichia coli*: old and new questions. *Mol Microbiol*. 1990;4(7):1063–7.
85. Dalbow DG, Young R. Synthesis time of β -galactosidase in *Escherichia coli* B/r as a function of growth rate. *Biochem J*. 1975;150(1):13–20.
86. Svenningsen SL, Kongstad M, Stenum TS, Muñoz-Gómez AJ, Sørensen MA. Transfer RNA is highly unstable during early amino acid starvation in *Escherichia coli*. *Nucleic Acids Res*. 2017;45(2):793–804.
87. Menninger JR. Accumulation of peptidyl tRNA is lethal to *Escherichia coli*. *J Bacteriol*. 1979;137(1):694–6.
88. Johnston TC, Borgia PT, Parker J. Codon specificity of starvation induced misreading. *Mol Genet MGG*. 1984;195(3):459–65.
89. Andersen C, Wiborg O. *Escherichia coli* elongation-factor-Tu mutants with decreased affinity for aminoacyl-tRNA. *Eur J Biochem*. 1994;220(3):739–44.
90. Bremer H, Dennis P. *Escherichia coli* and *Salmonella*: cellular and molecular biology. Washington, DC: American Society for microbiology chapter, modulation of chemical composition and other parameters of the cell by growth rate; 1996. p. 1553–69.
91. Miyajima A, Kaziro Y. Coordination of levels of elongation factors Tu, Ts, and G, and ribosomal protein S1 in *Escherichia coli*. *J Biochem*. 1978;83(2):453–62.
92. King EO, Ward MK, Raney DE. Two simple media for the demonstration of pyocyanin and fluorescin. *J Lab Clin Med*. 1954;44(2):301–7.
93. Deng C-Y, Deng A-H, Sun S-T, Wang L, Wu J, Wu Y, et al. The periplasmic PDZ domain-containing protein Prc modulates full virulence, envelops stress responses, and directly interacts with dipeptidyl peptidase of *Xanthomonas oryzae* pv. *oryzae*. *Mol Plant Microbe Interact*. 2014;27(2):101–12.
94. Boucher CA, Barberis PA, Trigalet AP, Demery DA. Transposon mutagenesis of *Pseudomonas solanacearum*: isolation of Tn5-induced avirulent mutants. *Microbiology*. 1985;131(09):2449–57.
95. Huynh TV, Dahlbeck D, Staskawicz BJ. Bacterial blight of soybean: regulation of a pathogen gene determining host cultivar specificity. *Science*. 1989;245(4924):1374–7.
96. Tsuge S, Furutani A, Fukunaka R, Takashi O, Tsuno K, Ochiai H, et al. Expression of *Xanthomonas oryzae* pv. *oryzae* *hrp* genes in XOM2, a novel synthetic medium. *J Gen Plant Pathol*. 2002;68(4):363–71.
97. Yoshimochi T, Zhang Y, Kiba A, Hikichi Y, Ohnishi K. Expression of *hrpG* and activation of response regulator HrpG are controlled by distinct signal cascades in *Ralstonia solanacearum*. *J Gen Plant Pathol*. 2009;75(3):196–204.
98. Schleif R, Hess W, Finkelstein S, Ellis D. Induction kinetics of the L-arabinose operon of *Escherichia coli*. *J Bacteriol*. 1973;115(1):9–14.

Publisher's Note

Springer Nature remains neutral with regard to jurisdictional claims in published maps and institutional affiliations.

Ready to submit your research? Choose BMC and benefit from:

- fast, convenient online submission
- thorough peer review by experienced researchers in your field
- rapid publication on acceptance
- support for research data, including large and complex data types
- gold Open Access which fosters wider collaboration and increased citations
- maximum visibility for your research: over 100M website views per year

At BMC, research is always in progress.

Learn more biomedcentral.com/submissions

